AIAA JOURNAL
Vol. 40, No. 3, March 2002

Aerodynamics of a Jet in the Vortex Wake of a Wing

Frank Y. Wang* and K. B. M. Q. Zaman†
NASA John H. Glenn Research Center at Lewis Field, Cleveland, Ohio 44135

Results of a low-speed experimental investigation of jet behavior in the trailing vortex wake of a wing are presented. The effects of varying jet-to-freestream velocity ratio and vortex-wake strength on the downstream evolution of the flowfield are quantified via three-dimensional hot-wire anemometry surveys. Under conditions encountered in powered flight, especially flow states characteristics of takeoff, landing, and maneuvering of a vehicle, the jet is found to undergo severe distortion within a very short distance from the nozzle exit. The interaction of the jet and the wing vortices generates additional vortical structures. Spreading and decay of the jet are shown to be governed predominantly by the interaction of the vortices.

Nomenclature

D	=	jet diameter
U_{jet}	=	jet bulk velocity
U_∞	=	freestream velocity
u, v, w	=	axial, transverse, and spanwise velocity components
$\overline{u'^2}, \overline{v'^2}, \overline{w'^2}$	=	mean squared axial, transverse, and spanwise velocity fluctuations
X, Y, Z	=	axial, transverse, and spanwise directions of Cartesian coordinates
α	=	planform angle of attack
Γ	=	circulation
ω_X	=	axial vorticity

Introduction

THE behavior of a propulsive jet behind aerodynamic planforms represents a subject of academic and practical interest because it has significance in many technological areas. For example, engine exhaust products entrained in the vortex wake would have different dispersion and mixing characteristics from those in a simple coflowing jet. Therefore, it is important to consider the effect of the aircraft vortex wake on the propulsive jet when assessing environmental impact from civil aviation activities.[1–3] In addition, the exhaust characteristics of military aircraft can also influence the target acquisition effectiveness of optically based sensors.[1,4,5] Furthermore, vortex–plume interactions modify the acoustics and mixing characteristics of high-speed jets,[5] a process that must be clearly understood to achieve accurate predictive capabilities. In spite of these practical considerations, as pointed out by Sforza,[6] studies on the subject had been very sparse at best. Thus, there exists a need for a robust experimental database to enhance physical understanding, as well as to facilitate code validation on the subject.

Experimentally, the earliest pertinent investigation appeared to be that of Werlé and Fiant, in 1964, who conducted flow visualization studies of jets issuing into the vortex wake of a Concorde-type planform.[7] In the side-view water-tunnel visualization presented by these authors, leading-edge vortices from the model were observed to be sometimes drawn into the simulated jet exhaust in the near field. However, spreading of the jet appeared similar to that of a freejet.

Received 8 January 2001; revision received 15 August 2001; accepted for publication 16 August 2001.

*National Research Council Research Associate, Nozzle Branch; currently Aerospace Engineer, John A. Volpe National Transportation Systems Center, Cambridge, MA 02142. Senior Member AIAA.

†Aerospace Engineer, Nozzle Branch. Associate Fellow AIAA.

Motivated by concerns regarding aircraft vortex-wake hazard in terminal area operations, El-Ramly and Rainbird[8] in 1977 carried out an investigation pertaining to the effect of engine exhaust on a wing tip vortex. The study included pitot pressure surveys of the exhaust at two and a half spans downstream of the trailing edge at angles of attack of 5 and 11 deg. The pitot pressure results for the Boeing 747 configuration examined revealed that engine exhausts did not appreciably influence the wing tip vortex structure but had profoundly altered the shear layer coming off the wing's trailing edge. Also, the trajectories and pitot pressure distributions of the exhausts were observed to be significantly affected.

In 1996, as part of a numerical investigation on the dynamics of a jet in aircraft vortex wakes, Jacquin and Garnier[9] presented a smoke visualization photograph of a jet exhaust behind a representative large transport aircraft at cruise conditions. A laser lightsheet was placed in the crossflow plane at one-half wingspan downstream. The visualization revealed a tear-drop-shaped plume, suggesting that part of the jet may have already been entrained into the wing vortex at a short distance downstream.

Seiner et al.[5] in 1997 presented their study of wing vortex-wake and pylon-wake influences on a high-speed subsonic round jet, with a particular focus on aeroacoustic implications. A straight half-wing fixed at 8-deg angle of attack, with a pylon-mounted axisymmetric nozzle underneath, was used in the investigation. Velocity distributions in the plume were mapped out using a multihole probe, while cold-wire and aspirated thermocouple probes were used to characterize the temperature field. Laser lightsheets were also utilized to help identify the trajectories of wing vortex and plume. These surveys were performed up to 100 jet diameters downstream. Numerical simulations using two different codes were also made, comparing favorably with the experiments. The results showed the jet evolved into a non-circular structure in the survey limits, and thus, they inferred that it would probably lead to a nonsymmetric noise field as well.

In 1999, in support of a three-dimensional direct numerical simulation (DNS) effort to quantify jet mixing behind aircraft, Brunet et al.[10] presented experimental results of a hot jet behind a generic wing planform. The jet to freestream velocity and temperature ratios were three and two, respectively. The wing was set at 9-deg angle of attack, with the jet oriented parallel to the freestream direction. Laser Doppler velocimetry and thermocouples were used to survey the jet at four locations, ranging from one-half to eight wing spans downstream. At half-span (or equivalently 25 jet diameters) away, their configuration led to an elliptically shaped jet. At three spans (or 150 jet diameters) downstream, ingestion of the jet by the wing tip vortex was observed. The DNS results are in qualitative agreement with the experiment, but primarily because of the low Reynolds number used, the simulation underestimated the jet plume mixing by the vortex wake.

Wang et al.[1] in 2000 presented their low-speed study on the evolution of a jet in the vortex wake of a simple delta wing. Laser lightsheet visualizations were performed for three planform angle-of-attack cases, that is, 5, 15, and 25 deg, and for three stations

at distances up to 111 jet diameters downstream. The flow visualization revealed substantial alteration in the jet cross section and suggested the existence of additional vortical structures around the jet. A two-dimensional version of the vortex-filament model, which included the assumption that the flow features in question around the jet were vortices, was shown to provide a reasonable qualitative description of the visualized flowfield. However, the assumptions introduced in the model and the details of the plume could not be resolved only with flow visualization data. Limited measurements in the jet were also made, in the form of centerline total pressure surveys for the $\alpha = 15$ deg case up to 34 jet diameters downstream. The results demonstrated that the velocity decay was much more rapid than that of a coflowing jet of the same velocity ratio.

The current study is an attempt not only to substantiate the jet flow physics postulated in Ref. 1, but to quantify it in detail as well. To accomplish this, a wind tunnel, which permitted the installation of a larger delta-wing/jet model, was employed. The investigation was restricted to the near field, considered to be the downstream distance of the exhaust before its ingestion into wing vortices. To isolate the influence of the vortex wake itself on the evolving plume, the orientation of the jet was fixed parallel to the freestream direction instead of varying with the planform's angle of attack.[1] The angle of attack and the jet-to-freestream velocity ratio were varied, and the associated three-dimensional flowfield was measured. Key results of the investigation are presented in the following.

Experimental Setup

The investigation was conducted in a 51×76 cm suction-type low-speed wind tunnel with a maximum speed of approximately 12 m/s. The nominal turbulence level in the test section is 0.1%. The schematic diagram of the jet–wing apparatus and the left-handed coordinate system employed are shown in Fig. 1.

A circular pipe of 19.1-mm inside diameter was introduced through the bottom floor of the tunnel. The pipe was first directed toward the inlet along the tunnel floor and then turned back, as shown in Fig. 1, thereby allowing the flow to pass through a long straight section before exhausting. The straight section was fitted with two flow conditioning screens (Fig. 1) to produce an axisymmetric flow at the pipe exit. The jet was supplied by shop air and controlled using a regulator. The mass flow of the incompressible jet was monitored with an orifice meter, from which the average velocity was inferred via the continuity relation.

The wing planform is flat-top delta wing with a 10-deg chamfer angle normal to its leading edges. The wing model has a 75-deg sweepback angle, a 127-mm span at the trailing edge, and a constant thickness equal to 1.6 mm. The wing was mounted over the jet orifice in a negative angle-of-attack orientation (Fig. 1). Throughout this investigation, the freestream velocity of the tunnel was fixed at 6.1 m/s.

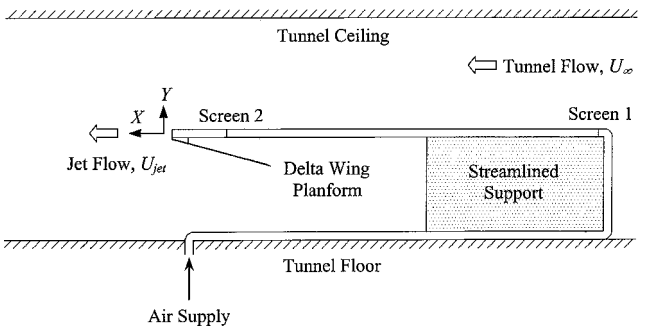

Fig. 1a Side-view schematic drawing of the experimental setup.

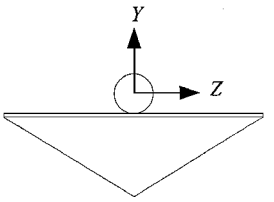

Fig. 1b Front-view schematic drawing of the jet and delta wing looking upstream.

Three-dimensional flow surveys were conducted using hot-wire anemometry. Two Dantec™-R51 X-wire probes mounted 18.3 mm apart on a computer-driven traverse were employed for the diagnostics, measuring the u–v and u–w components, respectively. The probes were moved in the wing spanwise direction so that they traversed through the same measurement locations but at different times, with redundancy in the u component for consistency check. At each measurement location, data acquisition was performed over 10 s at a sampling rate of 1000 Hz. Further details on the hot-wire data acquisition and reduction are found in Ref. 11.

Results and Discussion

Coflowing Jet Baseline Case

Before the introduction of the wing planform, characteristics of the coflowing jet itself were investigated for U_{jet}/U_∞ ratios of 2 and 4. Each velocity ratio setting involved six survey stations, ranging from 1 to 21 jet diameters downstream as permitted by the existing tunnel configuration. The location of maximum jet velocity at the one-diameter downstream location was first determined by surveying the flowfield using spatial increments of 0.25 mm. This maximum velocity location was referenced as the coordinate origin for the surveys (Fig. 1). Thereafter, a spatial resolution of 3.05 mm in both horizontal and vertical traverses was employed throughout the data acquisition. This resolution represented 2.4 and 16% of the span and jet diameter, respectively. An example of the normalized velocity distribution, defined as $(u^2 + v^2 + w^2)^{0.5}/U_\infty$, is shown in Fig. 2. It can be seen that the jet cross section is axisymmetric and that the jet axis is aligned with the geometric axis. The planform was next introduced such that its trailing edge rested on the same cross-sectional plane as the jet exit (Fig. 1). The experiments involved three jet-to-freestream velocity ratios of 0, 2, and 4, and three planform angles of attack of 5, 15, and 20 deg. For each combination of these two parameters, measurements at the same six downstream locations were repeated. However, the symmetry condition was utilized, and the survey limits at each station were shifted toward the starboard side. The Reynolds number of the delta wing planform based on the root chord was 1.0×10^5. For the jet, the Reynolds numbers at velocity ratios of 2 and 4 based on the orifice diameter were, respectively, 1.6×10^4 and 3.2×10^4.

Velocity Distribution

The results for the $\alpha = 15$ deg and jet-to-freestream velocity ratio of 4 case are first discussed. Figure 3 shows contours of time-averaged total velocity for the six downstream survey locations. The tip of the planform trailing edge is located at $Z/D = 3.33$, $Y/D = 0.54$. It is clearly seen that the presence of the planform significantly deforms the jet. Specifically, the jet is increasingly stretched sideways while compressed vertically. Moreover, for distances up to nine jet diameters, an indentation in the jet cross section is observed at approximately the two o'clock position.

Using the $\alpha = 15$ deg and jet-to-freestream velocity ratio of 4 case as a reference, results for other conditions are discussed in the following. Figure 4 summarizes the velocity distribution for various combinations of test conditions at nine jet diameters downstream.

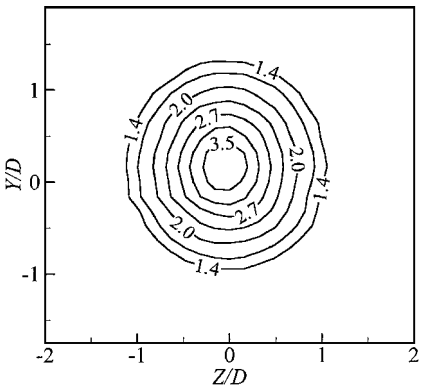

Fig. 2 Normalized velocity for the coflowing jet setup at nine jet diameters and $U_{jet}/U_\infty = 4$.

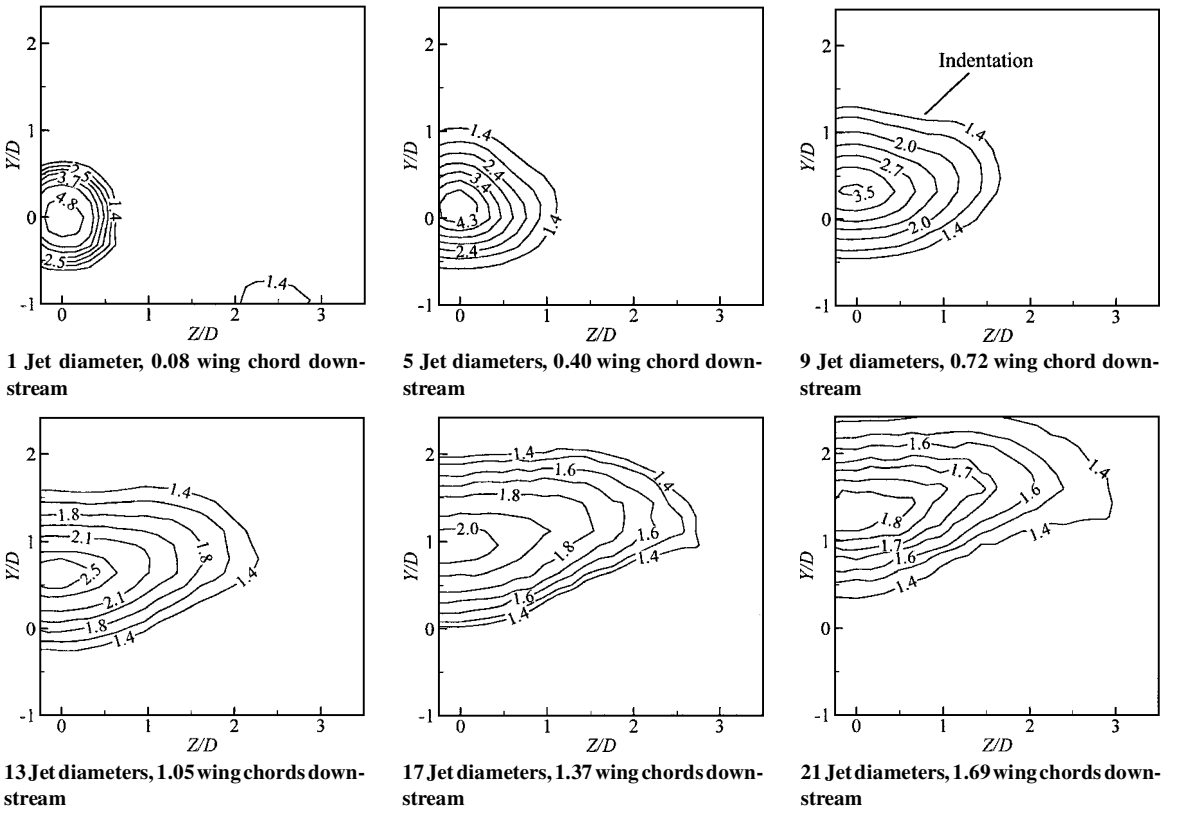

1 Jet diameter, 0.08 wing chord downstream

5 Jet diameters, 0.40 wing chord downstream

9 Jet diameters, 0.72 wing chord downstream

13 Jet diameters, 1.05 wing chords downstream

17 Jet diameters, 1.37 wing chords downstream

21 Jet diameters, 1.69 wing chords downstream

Fig. 3 Normalized velocity contours for $\alpha = 15$ deg, $U_{jet}/U_\infty = 4$ case.

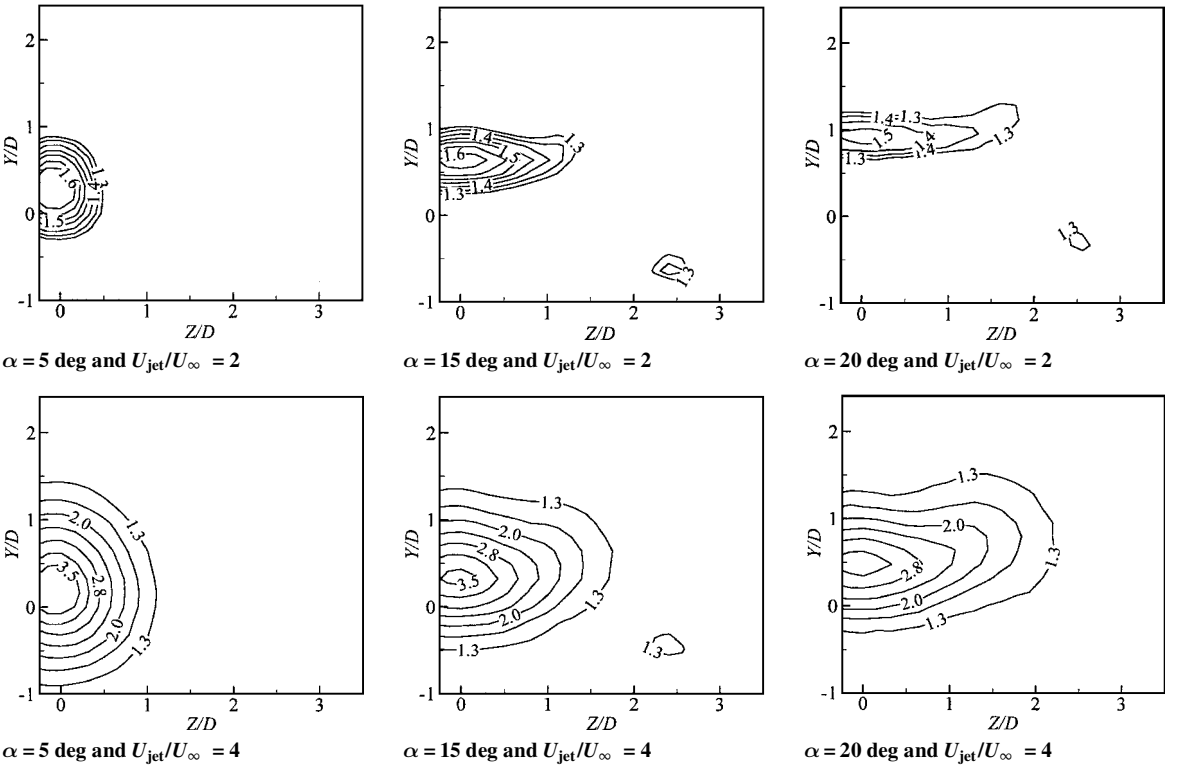

$\alpha = 5$ deg and $U_{jet}/U_\infty = 2$

$\alpha = 15$ deg and $U_{jet}/U_\infty = 2$

$\alpha = 20$ deg and $U_{jet}/U_\infty = 2$

$\alpha = 5$ deg and $U_{jet}/U_\infty = 4$

$\alpha = 15$ deg and $U_{jet}/U_\infty = 4$

$\alpha = 20$ deg and $U_{jet}/U_\infty = 4$

Fig. 4 Normalized velocity contours at 9 jet diameters downstream for various α and U_{jet}/U_∞ combinations.

From these, the severity of the indentation is seen to increase with increasing angle of attack and with decreasing jet velocity ratio. The aforementioned trends hold with the exception of the 5-deg angle-of-attack cases, in which the jet remained approximately round. This exception will be revisited later in the paper.

The maximum jet axial velocity, normalized by the corresponding maximum velocity for the coflowing jet without the wing at one diameter, is summarized in Fig. 5. Compared to the no-wing baseline cases, jets in the vortex wake of a planform decay substantially faster and earlier. Note that in the presence of the wing, the maximum velocity of the jet is not always along the $Z = 0$ axis. Instead, the location of maximum jet velocity can migrate toward the leading-edge vortex in certain cases, causing the velocity along the axis of symmetry to be lower. It appears that when the jet becomes weaker, the streamwise vortices from the wing start tearing the jet so that its maximum velocity location is driven off the $Z = 0$ axis. Among the cases examined, the jet in the 13–21-diameter range for the combination of $\alpha = 20$ deg and jet-to-freestream ratio of 2 has

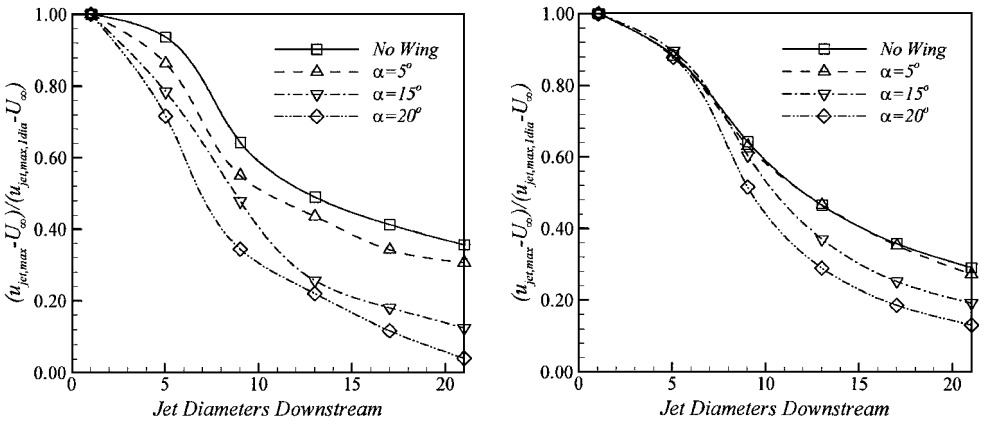

$U_{jet}/U_\infty = 2$ $U_{jet}/U_\infty = 4$

Fig. 5 Axial jet velocity decay characteristics.

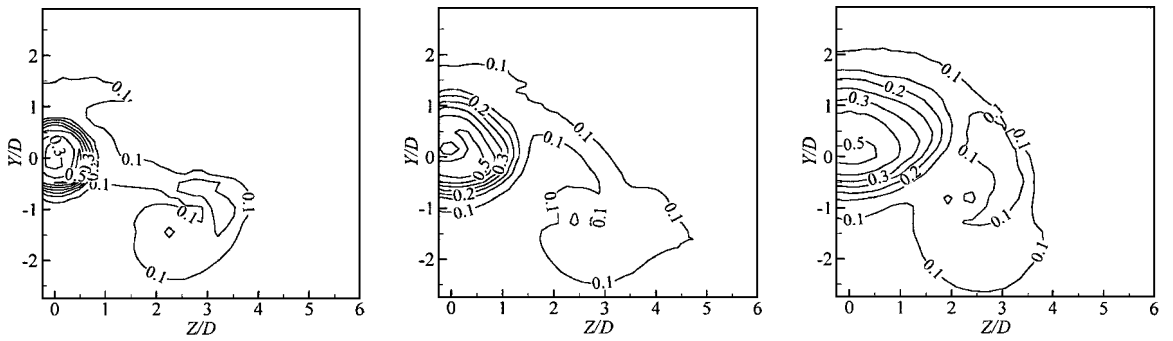

1 Jet diameter, 0.08 wing chord downstream **5 Jet diameters, 0.40 wing chord downstream** **9 Jet diameters, 0.72 wing chord downstream**

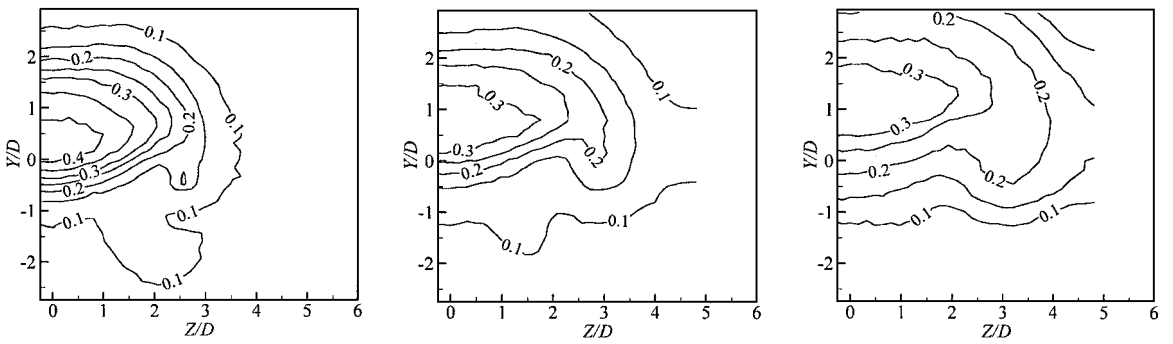

13 Jet diameters, 1.05 wing chords downstream **17 Jet diameters, 1.37 wing chords downstream** **21 Jet diameters, 1.69 wing chords downstream**

Fig. 6 Turbulence intensity contours for $\alpha = 15$ deg, $U_{jet}/U_\infty = 4$ case.

the maximum velocity located away from the $Z = 0$ axis. Thus, if jet decay were characterized by the maximum velocity along the $Z = 0$ axis, the curve for the $\alpha = 20$ deg and jet-to-freestream ratio of 2 combination in Fig. 5 would have decreased even further from 13 diameters and beyond.

Turbulence Intensity

The turbulence intensity characteristics of the jet, defined herein as $\sqrt{[\frac{1}{3}(\overline{u'^2}+\overline{v'^2}+\overline{w'^2})]}/U_\infty$, are next examined. Data corresponding to the cases of Fig. 4 are shown in Fig. 6. Between 5 and 13 diameters downstream, the highest turbulence intensity region is found in the lower part of the jet, that is, shifted toward the incoming upwash of the leading-edge vortices. Associated with this redistribution of turbulence intensity, generally a slightly higher level compared to the no-wing baseline case is also noted. The streamwise variation of the maximum turbulence intensity corresponding to the cases of Fig. 5 is summarized in Fig. 7. Note that the seemingly high values of turbulence intensity resulted from the normalization with respect to the freestream velocity, instead of the bulk velocity of the jet.

Axial Vorticity

Distributions of streamwise vorticity, normalized as $\omega_X D/U_\infty$, are examined next. A set of reference data involving the planform at the various angles of attack without activating the jet were first taken. Representative data for the $\alpha = 15$ deg case are shown in Fig. 8. The anticipated flow topology behind a delta wing[12] comprises pairs of leading-edge (also known as the primary) and secondary vortices. Both vortical features can be seen at one jet diameter downstream in Fig. 8. The vorticity sheet from the trailing edge of the planform is likewise discernible at this location. By nine jet diameters downstream, the shear layer off the trailing edge and the secondary vortex of the delta planform have decayed significantly, leaving the leading-edge vortex as the dominant feature thereafter.

With the jet activated, as shown in Fig. 9, a vorticity sheet of positive sign in the vicinity of the jet boundary is evident. This strip of vorticity is observed to roll quickly into an additional concentrated vorticity region above the jet. The position of the concentrated vorticity is in the same general vicinity as that of the indentation in the jet shown in Fig. 3. The crossflow velocity field also revealed

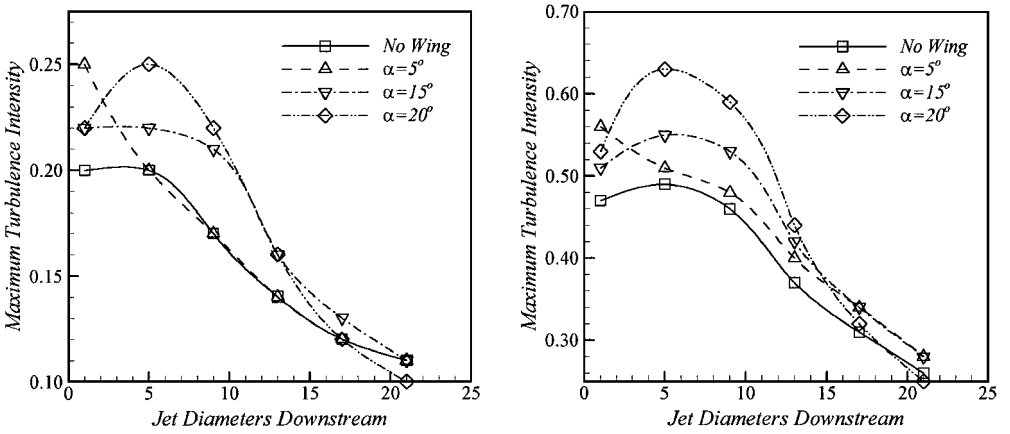

U_{jet}/U_∞ = 2 case U_{jet}/U_∞ = 4 case

Fig. 7 Summary of centerline maximum turbulence intensity level in the jets.

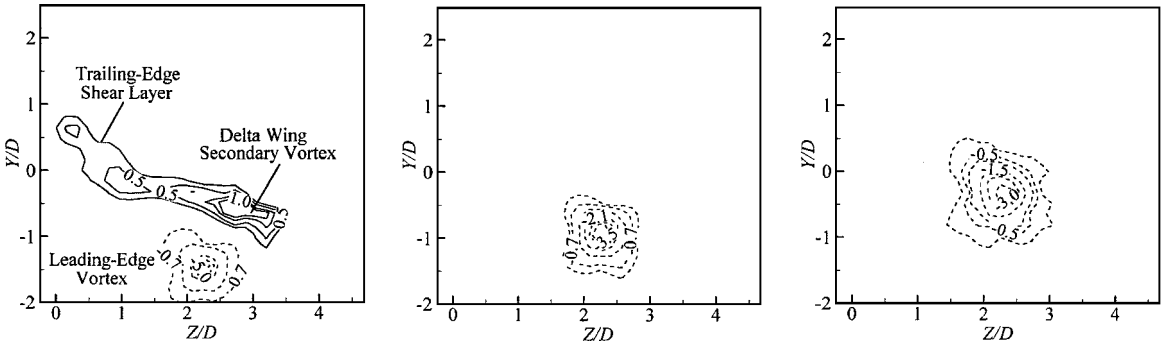

1 Jet diameter, 0.08 wing chord downstream **9 Jet diameters, 0.72 wing chord downstream** **17 Jet diameters, 1.37 wing chord downstream**

Fig. 8 Normalized axial vorticity contours for $\alpha = 15$ deg, $U_{jet}/U_\infty = 0$ case.

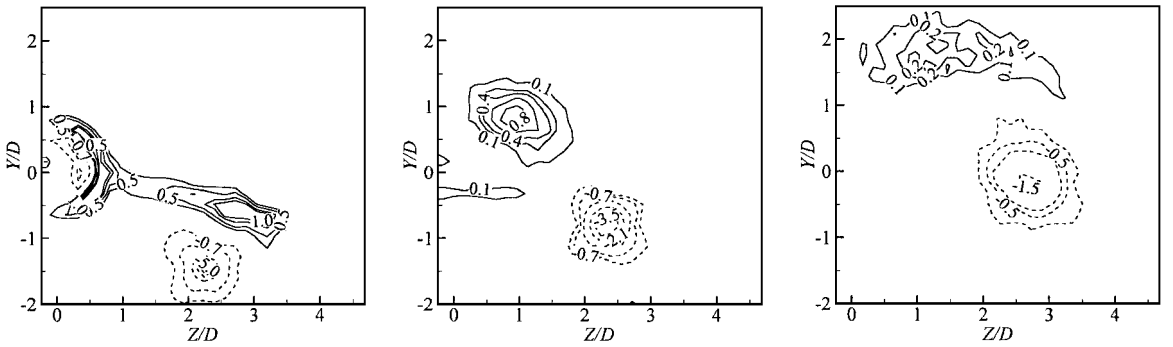

1 Jet diameter, 0.08 wing chord downstream **9 Jet diameters, 0.72 wing chord downstream** **17 Jet diameters, 1.37 wing chord downstream**

Fig. 9 Normalized axial vorticity contours for $\alpha = 15$ deg, $U_{jet}/U_\infty = 4$ case.

a swirling pattern in the area of the concentrated positive vorticity region. This region of positive vorticity will be referred to as the jet vortex hereafter. The maximum magnitude of this vorticity at a given downstream location was found to increase with increasing angles of attack, as well as with increasing jet-to-freestream velocity ratio. With a fixed angle of attack and a given jet velocity, the vorticity associated with the jet also decayed rapidly with distance downstream. However, unlike the secondary vortex stemming from the delta wing planform, this newly produced vortex system persisted farther and was discernible even at 17 diameters downstream (Fig. 9). With the exception of the $\alpha = 5$ deg and $U_{jet}/U_\infty = 4$ case, the aforementioned description of the vorticity field is generic. In addition to not having the deformed shapes in the mean velocity contour (Fig. 4), the vorticity field for the $\alpha = 5$ deg and $U_{jet}/U_\infty = 4$ case did not exhibit the additional well-organized and concentrated (positive) vorticity. The flowfield behaved as if it were simply a coflowing jet.

The mechanism by which the additional vortical feature over the jet is formed may be postulated as follows. As the high-momentum fluid issues from the jet orifice, it is immediately subjected to an upwash field from the wing planform in the experiment. The situation is then similar to that of a jet in a weak crossflow. In such a situation, a pair of bound vortices around the jet is formed and subsequently convected away.

While moving downstream, the jet vortices also interact with leading-edge vortices of the delta wing such that, acting together, they produce the jet distortion observed in Fig. 3. The development of the jet is, thus, believed to be heavily influenced by the dynamics of both leading-edge vortices from the delta wing and jet vortices.

However, should the momentum of the jet be too strong compared to that of the crossflow, the jet would then simply behave as if there was no crossflow, as was the case at $\alpha = 5$ deg and $U_{jet}/U_\infty = 4$. Consequently, no organized vortices are developed around the jet to create the localized distortion observed in the remaining cases of the test matrix. It is, however, speculated the jet in the $\alpha = 5$ deg and $U_{jet}/U_\infty = 4$ case would not remain unaffected, or round, throughout its lifespan in the vortex wake of the delta wing. Once the jet has decayed sufficiently and provided that it has not been ingested by the wing vortices, the dynamics of the vortex wake would again take effect and distort the jet in the manner described earlier.[1]

Circulation

For the cases in which very distinctive and concentrated vorticity regions are associated with the jet vortex, an attempt has been made to quantify its strength in terms of circulation. This was accomplished by line integration around a square grid with the maximum vorticity location as the center. The results were then normalized by the respective circulation of the leading-edge vortex (reduced from the velocity field in the same manner) at the one-diameter downstream location with the jet off. Figure 10 summarizes these results, and it is noted that, as jet velocity increases at a given angle of attack, there exists a corresponding increase in the jet circulation. At high angle of attack and high jet velocity, the circulation of the jet vortex in the present experimental arrangement is quite significant, but still weaker than that of the leading-edge vortex.

In the majority of the cases examined, although the jet is seen to be heavily influenced by the leading-edge vortex from the delta wing, the leading-edge vortex is not very much affected by the jet. However, if the jet momentum remains high while being ingested, a dramatic reduction in the circulation level of the leading-edge vortex is observed. When $\alpha = 15$ deg is used as an example, the decline in the leading-edge vortex strength is summarized in Fig. 11. Such a trend is consistent with the literature that shows pneumatic injection into the wing vortices attenuates their strength.[13–15]

Simulation of Jet Behavior

In light of the vortex-dominated features stemming from a jet issuing into the near-field wake of an aircraft planform, an analytical model was devised to facilitate the interpretations of experimental results. The details of the modeling are found in Ref. 1, and therefore, only a description of its basic premise is given here. In brief, the development of the jet is treated by reducing the problem to the interaction between leading-edge vortices generated by the delta wing and the jet vortices. The induced flowfield between these two pairs of vortices was calculated using a two-dimensional vortex filament approach,[1] which may also be known as the point vortex method. The evolution of the jet is then delineated by following the trajectories of a ring of tracer particles (modeled as vortices of zero circulation) from the jet exit. For further simplicity, the jet momentum and its natural spreading have been neglected. The modeling requires no input from experiments. However, a minor adjustment in the formulation was made to reflect the orientation of the jet in the current experiment. A representative calculation for the current experimental configuration at $\alpha = 15$ deg and nine diameters downstream is shown in Fig. 12. It suggested that the jet would evolve from a circular shape at the orifice to a horizontally elongated profile. The area between the two jet vortices has a shape that resembles a "w" and ascends qualitatively in a manner similar to that found in the measurements. Specifically, the jet vortices move up and away with respect to the jet orifice. A corresponding behavior is also noted for leading-edge vortices, which moved up and away from the jet. Their trajectories are also shown in Fig. 12. In comparison, if the calculation were performed without modeling the jet vortices, the outcome is presented in Fig. 13. Note that, in such a case, the

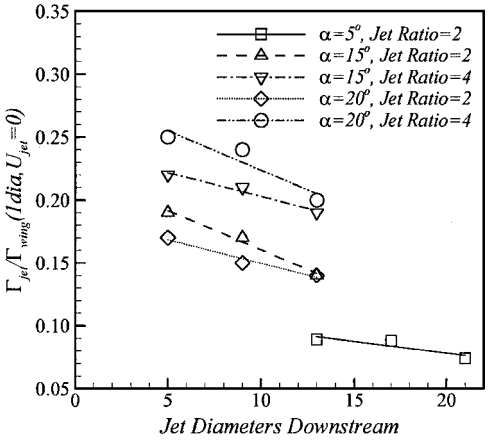

Fig. 10 Normalized circulation of jet vortices at various angles of attack.

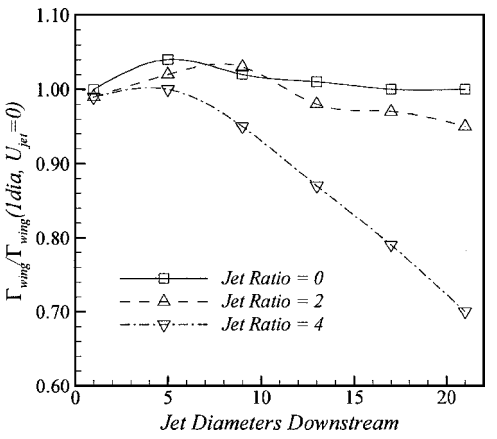

Fig. 11 Effect of U_{jet}/U_∞ on the $\alpha = 15$ deg leading-edge vortex circulation development.

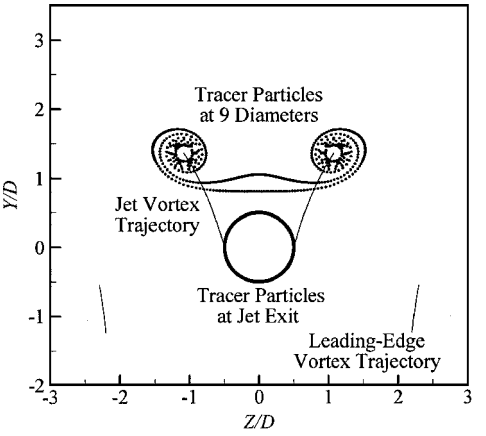

Fig. 12 Results of the calculation with modeling of jet vortices: $\alpha = 15$ deg at nine jet diameters downstream.

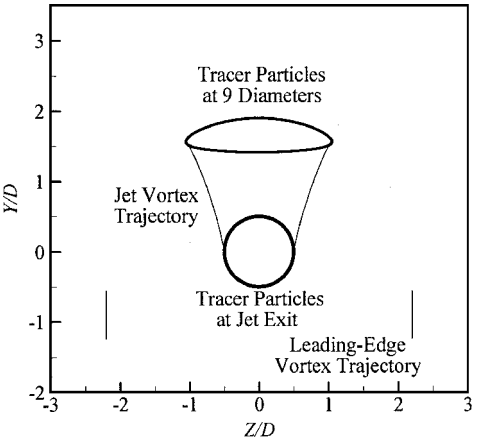

Fig. 13 Results of the calculation without modeling of jet vortices: $\alpha = 15$ deg at nine jet diameters downstream.

jet does not deform into the shape observed in the experiment. This exercise illustrates the critical influence of the jet vortices on the shape of the flowfield. The notion that the deformation of the jet seen in the experiment as being largely due to the dynamics of jet and leading-edge vortices is, thus, substantiated.

Summary

An experimental investigation on the aerodynamics of a propulsive jet in a forward flight condition has been presented. The study was performed in incompressible flow, and it involved immersing the jet in the vortex wake of a delta wing planform. The effects of varying vortex-wake strength and exit velocity on the downstream evolution of the jet were quantified via three-dimensional hot-wire anemometry surveys. In addition, interpretation of the experimental results was aided by an analytical model based on the interaction of discrete vortices.

It is shown that when vortices shed from airframe components pass by the vicinity of the jet (such as those from flaps, ailerons, strakes or fuselage junction, etc., during takeoff, landing and violent maneuvers of a flight vehicle) the jet could have a behavior quite different from that of an isolated coflowing jet. A salient feature of the jet, as a consequence of being immersed in the induced velocity field of the vortex wake of airframe vortices, is to produce additional vortices. The existence of these additional vortical structures that arise from the jet has been conclusively verified and quantified in the current investigation. The strength of these jet vortices has been shown to be rather significant. Given this, within a few diameters downstream from its exit, the jet would deform into a shape predominantly governed by the induced velocity fields of various vortices that surround it. In the present configuration, the jet experiences both lateral stretching and vertical compression due to the dynamics of its neighboring vortices and, ultimately, has a far quicker maximum velocity decay compared to that of the baseline coflowing jet of the same velocity ratio. In the process, the turbulence intensity field is also profoundly affected, and the maximum turbulence intensity location is shifted toward the incoming upwash region of the leading-edge vortices.

The trajectories of leading-edge vortices in the present experiment have been shown to be influenced slightly by the jet, again in a manner that could be accounted for by vortex dynamics. Moreover, if the leading-edge vortices begin to ingest a jet possessing a rather high momentum, the peak vorticity and circulation of the leading-edge vortices are shown to be substantially reduced.

Acknowledgments

This work was performed while the first author held a National Research Council Research Associateship Award at NASA John H. Glenn Research Center. The first author also wishes to thank Pasquale M. Sforza of the University of Florida for many helpful discussions and Michael M. J. Proot of Delft University of Technology for his help with the simulation model.

References

[1]Wang, F. Y., Proot, M. M. J., Charbonnier, J.-M., and Sforza, P. M., "Near-Field Interaction of a Jet with Leading Edge Vortices at Low Speed," *Journal of Aircraft*, Vol. 37, No. 5, 2000, pp. 779–785.

[2]Menon, S., and Wu, J., "Effect of Micro- and Macroscale Turbulent Mixing on the Chemical Processes in Engine Exhaust Plumes," *Journal of Applied Meteorology*, June 1998, pp. 639–654.

[3]Danilin, M. Y., Rodriguez, J. M., Ko, M. K. W., Weisenstein, D. K., Brown, R. C., Miake-Lye, R. C., and Anderson, M. R., "Aerosol Particle Evolution in an Aircraft Wake: Implications for the High-Speed Civil Transport Fleet Impact on Ozone," *Journal of Geophysical Research*, Vol. 102, No. D17, 1997, pp. 21,453–21,463.

[4]Dash, S. M., and Kenzakowski, D. C., "Hot Jet/Wake Turbulent Structure and Laser Propagation: Part I—Jet/Wake Turbulence Modeling," *Proceeding of the 21st Joint Army–Navy–NASA–Air Force (JANNAF) Exhaust Plume Technology Subcommittee Meeting*, Vol. 1, 1994, pp. 59–78.

[5]Seiner, J. M., Ponton, M. K., Jansen, B. J., Dash, S. M., and Kenakowski, D. C., "Installation Effects on High Speed Plume Evolution," American Society of Mechanical Engineers, ASME Paper FEDSM 97-3227, 1997.

[6]Sforza, P. M., "Interaction of Wing Vortices and Plumes in Supersonic Flight," *Proceedings of the IUTAM Symposium on Dynamics of Slender Vortices*, Kluwer Academic, Norwell, MA, 1998, pp. 415–424.

[7]Werlé, H., and Fiant, C., "Water-Tunnel Visualization of the Flow Around the Model of a 'Concorde'-Type Airplane," *La Recherche Aérospatiale*, Vol. 102, 1964, pp. 3–19.

[8]El-Ramly, Z., and Rainbird, W. J., "Effect of Simulated Jet Engines on the Flowfield Behind a Swept-Back Wing," *Journal of Aircraft*, Vol. 14, No. 4, 1977, pp. 343–349.

[9]Jacquin, L., and Garnier, F., "On the Dynamics of Engine Jets Behind a Transport Aircraft," *The Characterisation & Modification of Wakes from Lifting Vehicles in Fluids*, CP-584, AGARD, 1996, pp. 37.1–37.8.

[10]Brunet, S., Garnier, F., and Jacquin, L., "Numerical/Experimental Simulation of Exhaust Jet Mixing in Wake Vortex," AIAA Paper 99-3418, 1999.

[11]Foss, J. K., and Zaman, K. B. M. Q., "Large- and Small-Scale Vortical Motions in a Shear Layer Perturbed by Tabs," *Journal of Fluid Mechanics*, Vol. 382, March 1999, pp. 307–329.

[12]Anderson, J. D., Jr., *Fundamentals of Aerodynamics*, 2nd ed., McGraw–Hill, New York, 1991, pp. 359–361.

[13]Poppleton, E. D., "Effect of Air Injection into the Core of a Trailing Vortex," *Journal of Aircraft*, Vol. 8, No. 8, 1971, pp. 672, 673.

[14]Kantha, H. L., Lewellen, W. S., and Durgin, F. H., "Response of a Trailing Vortex to Axial Injection into the Core," *Journal of Aircraft*, Vol. 9, No. 3, 1972, pp. 254–256.

[15]Snedeker, R. S., "Effect of Air Injection on the Torque Produced by a Trailing Vortex," *Journal of Aircraft*, Vol. 9, No. 9, 1972, pp. 682–684.

A. Plotkin
Associate Editor